Platelet rich plasma enhanced neuro-regeneration of human dental pulp stem cells *in vitro* and in rat spinal cord

Zi-Bing Hu[1], Hai-Cong Chen[1], Bo Wei[1], Zhong-Min Zhang[2], Shao-Ke Wu[1], Jie-Cong Sun[1], Min Xiang[1]

[1]Orthopedic Center, Affiliated Hospital of Guangdong Medical University, Zhanjiang, China; [2]Spinal Surgery, Nanfang Hospital of Southern Medical University, Guangzhou, China

Contributions: (I) Conception and design: ZB Hu, ZM Zhang; (II) Administrative support: ZB Hu, B Wei; (III) Provision of study materials or patients: ZM Zhang, HC Chen; (IV) Collection and assembly of data: SK Wu, JC Sun; (V) Data analysis and interpretation: ZB Hu, M Xiang; (VI) Manuscript writing: All authors; (VII) Final approval of manuscript: All authors.

Correspondence to: Zi-Bing Hu, PhD. Orthopedic Center, Affiliated Hospital of Guangdong Medical University, Zhanjiang, China. Email: zibinghu@gdmu.edu.cn.

Background: Human dental pulp stem cells (hDPSCs) exhibit excellent differentiation potential and are capable of differentiating into several different cellular phenotypes, including neurons. Platelet-rich plasma (PRP) contains numerous growth factors that can stimulate stem cell differentiation. In this study, we investigated the potential stimulatory effects of PRP on neurogenic differentiation and anti-apoptosis of hDPSCs in injured spinal cords.

Methods: The unipotential differentiation capacity of hDPSCs was analyzed by cell surface antigen identification and cell cycle analysis. A spinal cord injury rat model composed of 40 Sprague-Dawley (SD) rats was used to facilitate an *in vivo* study. Rats were divided into four groups: a double-treatment group (receiving both neurogenic-induced hDPSCs and PRP), two single-treatment groups (receiving neurogenic-induced hDPSCs or PRP) and a sham group (receiving normal saline). The Basso, Beattie, Bresnahan Locomotor Rating Scale was subsequently used to evaluate the motor function of the spinal cord. Cell viability and differentiation of hDPSCs in the damaged spinal cords were analyzed and apoptosis of neural cells was evaluated using the terminal uridine nucleotide end labeling (TUNEL) assay.

Results: Growth pattern, cell surface marker and cell cycle analyses revealed that hDPSCs have a high degree of multi-directional differentiation potential and can be induced into neurons *in vitro*. In the rat spinal cord injury model, double-treatment with hDPSC/PRP or single treatment with hDPSCs or PRP significantly improved motor function compared with the sham group (P<0.05). Apoptosis of neural cells was observed to be significantly higher in the sham group compared to any of the treatment groups. Double-treatment with hDPSCs and PRP resulted in the lowest apoptotic rate among the groups analyzed.

Conclusions: hDPSCs exhibit differentiation potential and are capable of transforming into neural cells both *in vitro* and *in vivo*. Significantly increased inhibition of neuronal apoptosis and improved motor function recovery of the spinal cord were observed following double-treatment with hDPSCs and PRP compared with the single-treatment groups.

Keywords: Human dental pulp stem cells (hDPSCs); spinal cord injury; platelet-rich plasma (PRP); apoptosis; neural differentiation

Page 2 of 12

Hu et al. PRP enhanced hDPSC neuro-regeneration

Introduction

Any insult to the spinal cord can result in the dramatic loss of motor, sensory, or autonomic functions with potential chronic pain or spasticity (1). It is estimated that the annual incidence of spinal cord injury, not including those individuals who die at the scene of accidents, is approximately 40 per million people in the United States, which equates to approximately 12,000 new cases per year (2). Some patients may exhibit partial spontaneous recovery after injury; however, damage to the spinal cord is usually permanent, as injured nerve cells cannot regenerate due to scar tissue formation and molecular processes inside the nerves (3). Additionally, damage to the spinal cord, whether caused by injury or disease, cannot currently be repaired by any therapy (4). Thus, spinal cord injury represents a major concern following traumatic events and effects patients' physical, psychological, and social wellbeing. Thus, this form of injury imposes a substantial financial burden on healthcare systems (5).

Despite the associated challenges, there is growing interest in the discovery of novel therapeutic strategies for effective spinal cord injury repair. Indeed, recent advances in regenerative and engineering therapies have provided novel insights into repair and suggest that the potential exists for improved repair strategies. In recent years, stem cell-based therapies have emerged as viable alternatives in spinal injury repair. It is recognized that damaged spinal cord tissues display a certain degree of plasticity whereby lost nerve cells can be replaced, and damaged neurons can be regenerated from stem cells (3,4,6). Research has shown that mesenchymal stem cells (MSCs)/progenitor cells, derived from mesodermal tissues, provide a potential source for neural regeneration (7). Human dental pulp stem cells (hDPSCs), one source of MSCs, can easily be collected from discarded permanent teeth and harvested in a minimally invasive manner. Due to their accessibility and ability to differentiate into several cellular phenotypes, including neurons, hDPSCs have been extensively studied in tissue engineering and regenerative medicine (8-11). HDPSCs have also been shown to have increased angiogenic, neurogenic, and regenerative potential. Thus, hDPSCs represent an attractive and versatile stem cell source for tissue engineering.

The ability of hDPSCs to differentiate into neurogenic cells *in vivo* is limited. For example, glial cells have been observed to function actively by secreting a large number of neurotrophic factors to facilitate nerve repair; however, rapid glial cell proliferation causes scar formation, which blocks nerve fiber growth and neuron-neuron connection (12). Thus, the induction and regulation of neuron growth, development, migration, survival, and apoptosis require the precise coordination of neurons and supporting cells by neurotrophic factors. Neurotrophic factors represent a class of secretory peptides produced by neuron innervated tissues and glial cells. These peptides play an important role in the induction and regulation of nerve cell growth, development, migration, survival, and apoptosis. A variety of neurotrophic factors have been identified, including nerve growth factor, neurotrophin-3, and neurotrophin-4 (13). However, as time has progressed, the possibility of a "single magic-bullet approach" for the treatment of neurodegenerative disorders has become unlikely. Indeed, emerging evidence suggests that a collection of multiple neurotrophic factors, most of which are unknown, are required to facilitate optimized treatment strategies (14).

Platelet-rich plasma (PRP) contains approximately 600 growth factors and cytokines that are primarily responsible for inducing differentiation, enhancing healing, and promoting tissue regeneration. This plasma source has become an attractive growth factor source in stem cell research (15-17) and is readily available for potential use in regenerative bone diseases. PRP also has a number of advantages related to the ease with which it can be isolated and handled, its enhanced storage properties, and its high effectiveness in bone tissue engineering. Additionally, PRP is autologous and does not represent a risk in relation to disease transmission or immune rejection.

Thus, to stimulate the ability of hDPSCs to differentiate into neurons while also elevating their inherent *in-vivo* survival capacity, we assessed the multipotency of hDPSCs. We also analyzed *in-vitro* neurogenic differentiation by introducing activated autologous PRP as a source of neurotrophic factors. We then observed the ability of PRP to promote the survival and neurogenic differentiation of hDPSCs in the injured spinal cords of rats. We present the following article in accordance with the ARRIVE reporting checklist (available at https://atm.amegroups.com/article/view/10.21037/atm-22-1745/rc).

Methods

Animals

Male Sprague-Dawley (SD) rats (aged 8 weeks, and weighing 200–220 g) were purchased from the Guangdong

Medical Laboratory Animal Centre and housed in a specific pathogen-free room at room temperature (22±1 ℃) under the relative humidity of 60–70% with free access to water and food. Animal experiments were performed under a project license (No. GDY1602042) granted by the institutional ethics committee of Guangdong Medical University (Zhanjiang, China), in compliance with national guidelines for the care and use of animals.

HDPSC cultures

The hDPSCs were provided by the Stomatological Hospital at Sun Yat-sen University. These 2nd generation hDPSCs had been isolated from the orthodontic 3rd molars of adults aged 18–28 years. The frozen hDPSCs were rapidly thawed in a preheated water bath and added to 10 mL of Dulbecco's Modified Eagle Medium (DMEM; Gibco, USA). After centrifugation and the removal of the supernatant, the cells were resuspended in DMEM supplemented with 10% fetal bovine serum (Guangzhou Chemical Reagent Company, China). After the viable cells were counted, they were seeded at a concentration of $1.0×10^6$ cells/mL into 25 cm^2 plastic flasks for culturing. The medium was changed every 3 days, and the cells were passaged when they reached 90% confluence. All samples were incubated at 37 ℃ in a 5% carbon diode (CO_2) humidified incubator.

Identification of hDPSC cell surface markers and cell-cycle analysis

The 4th-generation hDPSCs were harvested during the logarithmic phase of growth with trypsin and resuspended in phosphate buffered solution (PBS). The cells were then divided into 4 tubes, each of which contained 0.5 mL of cell suspensions (at a density of $1×10^7$ cells/0.5 mL). Next, 5 µL of mouse anti-human CD44-APC (Cluster of differentiation 44 allophycocyanin), CD34-FITC (Cluster of differ-entiation 34 fluorescein isothiocyanate), and CD146-PE (Cluster of differ-entiation 146 phycoerythrin) antibodies (BioLegend) were added to 1 of the tubes, and 5 µL of the 3 corresponding positive control antibodies were added to a 2nd tube. In a similar manner, 5 µL of mouse anti-human CD90-APC (Cluster of differ-entiation 90 allophycocyanin), STRO-1-FITC (Stromal cell antigen -fluorescein isothiocyanate), and CD45-PE (Cluster of differ-entiation 45 phycoerythrin) antibodies (BioLegend), and 5 µL of the corresponding positive controls were aliquoted into the remaining 2 tubes, respectively. The cells

were incubated for 30 min at 4 ℃ in the dark. Next, the cells were washed twice following centrifugation at 1,000 r/min for 5 min and resuspended in 0.5 mL of PBS. The cells were then transferred into flow cytometry test tubes to facilitate flow cytometry detection (BD, USA) of cell surface antigen expression.

The 4th-generation hDPSCs were also harvested for a cell-cycle analysis using flow cytometry. After the cells had been washed 3 times with PBS, 70% cold ethanol was added to fix the cells. A total of 0.2 mg of ribonuclease was subsequently added, and the cells were stained with 1 mL of PI/Triton X-100 staining solution (20 µg PI/0.1% Triton X-100). The cells were resuspended in PBS at 37 ℃ for 30 min. The cells were then transferred into flow cytometry test tubes for the cell-cycle analysis.

Neural induction assay

The 4th-generation hDPSCs were harvested at the logarithmic growth phase, digested in 4% trypsin, centrifuged, and counted. A total of $1×10^4$ cells were seeded into a glass bottom dish for confocal microscopy. Next, 1 mL of nerve induction medium (1% B27, 1% ITS, and 100 ng/mL of bFGF) was added to the cultured cells. The cells were further incubated at 37 ℃ in a 5%-CO_2 saturated-humidity incubator. Half of the medium was changed every 3 days, and the cultures were incubated for up to 14 days. Following the final incubation, the medium was removed, and the cells were washed 3 times with PBS (5 min per wash). Next, the cells were fixed in 4% paraformaldehyde (PFA) at room temperature for 15 min. The cells were then permeabilized in 0.2% Triton X-100 for 5 min. After blocking in 4% bovine serum albumin (BSA) at room temperature for 20 min, the cells were incubated overnight at 4 ℃ with 50 µL of NeuN and GFAP (rabbit anti-human IgG, 1:200) antibodies. This mixture was subsequently incubated for 2 h at 37 ℃ in a humid chamber. The cells were then incubated with 50 µL of anti-rabbit IgG-FITC antibody at a 1:48 dilution. Next, the cells were incubated in a humidified box at 37 ℃ for 3 hours. After several washes with PBS, the cells were observed and photographed under a Leica TCS SP5 II laser scanning confocal microscope.

For the flow cytometry study, the 4th-passage hDPSCs were cultured and harvested as described above. These cells were then seeded into a culture flask at a density of $1×10^6$ cells/bottle, and 5 mL of neural induction medium was added to each flask. These mixtures were cultured in a 5%-CO_2/100% water-saturated humidity incubator.

Page 4 of 12

Hu et al. PRP enhanced hDPSC neuro-regeneration

Using non-induced hDPSCs as a control, flow cytometry was performed. In brief, the cells with or without neural induction were harvested in trypsin and suspended in 1 mL of PBS. A total of 5 µL of nestin-PE antibody was added to the latter resuspensions, and the resultant mixtures were incubated at 4 ℃ for 30 min. After 2 washes in PBS, the cells were resuspended in 0.5 mL of PBS in flow cytometry dedicated test tubes. These tubes were used to facilitate the flow cytometry analysis of cell surface antigen expression.

Preparation of PRP

In this study, 3 SD rats were anesthetized with 7% chloral hydrate (0.3 mL/100 g) intraperitoneally. Next, 10 mL of blood was collected in a tube containing sodium citrate following the abdominal aorta puncture of each rat. The modified Appel method was used to prepare the PRP. In brief, after gentle mixing, the whole blood was centrifuged at 220 g for 20 min, and the supernatant was further centrifuged at 480 g for 20 min. The lower layer of sediment (containing PRP) was collected. Every 0.4 mL of platelets that were harvested were diluted in 1 mL of whole blood or PRP. These mixtures were rigorously shaken and incubated at room temperature for 5 min. After a transparent solution was obtained, a single drop of the resultant mixture was used to count the platelets under a microscope.

Preparation of acute spinal cord injury model in rats

The acute spinal cord injury rat model was prepared using a modified version of the Allen method. In brief, the rats were anesthetized [using an intraperitoneal injection of 7% chloral hydrate (0.3 mL/100 g)] and fixed on the surgical table. The T9–T12 vertebrae were exposed following a median incision. The T10 vertebra was partially removed to expose the spinal cord and dura. Each rat was fixed on a compression device. A stainless-steel column weighing 10 g with a diameter of 2.5 mm was dropped freely from a height of 4 cm. The column was subsequently left for 5 min, and the resultant impact area was approximately 2.5 mm × 2.5 mm. The incision was then closed layer by layer. Postoperatively, the rats were housed at room temperature with normal access to food and water. The rats were subsequently administered 120,000 U of penicillin per day by intramuscular injection. The rat bladders were massaged once or twice daily until bladder function recovered.

Injection of hDPSCs and PRP into rat spinal cords and Basso, Beattie, and Bresnahan (BBB) scoring

At 3 days post-operation, the animals were randomly divided into the following 4 treatment groups: (I) a double-treatment group in which the rats were administered both hDPSCs and PRP (n=13); (II) a single-treatment group in which the rats were administered hDPSCs (n=13); (III) a single-treatment group in which the rats were administered PRP (n=7); and (IV) a sham group in which the rats were administered normal saline (n=7). The rats were anesthetized and fixed as described above. Following a posterior median incision to expose the spinal cord and dura, the hDPSCs were injected at a concentration of 2.5×10^5 cells/2.5 µL in PBS into rats from appropriate groups using a Hamilton needle. The injections were administered at 4 different sites around the injured spinal cord at an injection depth of 1.5 mm. Next, 10 µL of PRP was injected into the injury sites of rats from the appropriate groups. Sterile normal saline was injected into rats from the sham group. Following each injection, the Hamilton needle was left for 5 min before removal. The incision was closed layer by layer. The postoperative rats were housed as describe above. The retention of hDPSC activity post-operation was analyzed following trypan blue staining.

Rat BBB scores were used to evaluate the motor function of the hind limbs according to the BBB Locomotor Rating Scale (18). The BBB scores were assessed by laboratory personnel (who were not familiar with the scoring system) on the day of modeling, 3 days after modeling, and 3, 7, 14, and 28 days after treatment.

H&E staining and cavity measurements of the spinal cords of the rats

In this study, 4 SD rats were chosen from each of the hDPSC/PRP, hDPSC, PRP, and sham groups. The rats were sacrificed at 4 weeks post-operation for hematoxylin and eosin (H&E) staining and cavity measurements. In brief, after routine anesthesia, the rats were fixed on the surgery table, and the hearts were exposed through rapid thoracotomy. The left ventricle was catheterized for rapid normal saline infusion. The rats were subsequently fixed via cold 4% PFA fixation solution infusion until the rats became stiff. A length of 10 mm spinal cord from the center of the injured site was harvested and fixed in 4% PFA at 4 ℃ for 4 hours. After routine dehydration using gradient ethanol solutions, the spinal cord was placed in alcohol-xylene for

5 min, and incubated in xylene I and II for 5 min, respectively. The spinal cord sections were subsequently embedded in paraffin. The samples were then sectioned (4-µm–thick sections) for routine H&E staining. An OLYMPUS DP71 microscopy system was used to facilitate the histological analysis and the calculation of the area of the syrinx.

Survival and differentiation of transplanted hDPSCs in the spinal cords

Following BBB scoring, the rats from the hDPSC/PRP and hDPSC groups were sacrificed at 3, 7, 14, and 28 days of treatment. The spinal cords of the sacrificed rats were harvested as described above. Next, the spinal cords were saturated overnight in 30% sucrose solution. The saturated samples were subsequently embedded in an optimal cutting temperature compound at –20 ℃, and frozen longitudinal sections (5-µm thick) were cut. Immunostaining was performed after blocking and permeabilizing the samples with 5% BSA and 0.2% Triton X-100 for 1 hour. The primary antibodies, GFAP-Hunu and NeuN-Hunu, were incubated overnight with the samples at 4 ℃. Next, sheep anti-rabbit-FITC and goat anti-mouse-Cyc3 secondary antibodies were added, and the resultant mixtures were incubated at room temperature. Finally, the samples were counterstained with 4',6-diamidino-2-phenylindole before observation under a confocal microscope.

TUNEL assay to assess apoptosis in spinal cord samples

Frozen sections from the hDPSC/PRP, hDPSC, PRP, and sham groups were used for the terminal deoxynucleotidyl transferase biotin-dUTP nick end labeling (TUNEL) apoptosis assay. The experiment was carried out in accordance with the instructions as set out in the manual of the TUNEL Apoptosis Assay Kit. From each spinal cord, 2 sections were randomly selected and 3 fields were visualized to count the apoptosis-positive cells.

Statistical analysis

SPSS17.0 was used for the data analysis. The BBB score, TUNEL cell apoptosis rate, and the percentage of syringomyelia were expressed as mean ± standard deviation ($\bar{x}±s$). Multiple comparisons were performed using a single-factor analysis of variance and the least-significant difference test.

Results

Characterization of in-vitro multipotent hDPSCs and neurogenic induction

Passaged homogeneous hDPSCs grew in a monolayer with spindle-shaped morphology from day 4 of the culture initiation (see *Figure 1A*). After 7 days, the cells proliferated rapidly and exhibited typical long spindle shapes. The cells were homogeneous in morphology, rich in cytoplasm, and had enlarged nuclei. In addition, the cells were arranged in a spiral or swirling parallel arrangement (data not provided). The cell morphology and growth rate did not differ significantly among the passages before passage 6 (data not provided). When the cells were passaged to the 10th generation or greater, signs of aging became apparent. The cells gradually appeared flat-shaped with pseudo-foot-like extensions and reduced proliferation (data not provided).

In relation to the cell surface markers, HDPSCs from different laboratories have been reported to express similar but non-specific patterns. This may be due to differences in tissue sources. The hDPSC expression patterns of the CD44, CD45, CD146, and STRO-1 surface antigens were tested using flow cytometry. The following expression profile was observed for the analyzed markers: CD34: 1.7%; CD45: 2.0%; STRO-1: 28.5%; CD146: 61.3%; and CD44: 99.6% (see *Figure 1B*). The results revealed excellent cell homogeneity, indicating that human 3rd molar pulp tissue culture cells exhibit similar characteristics to those of hDPSCs. The flow cytometry analysis confirmed the following cell-cycle profile for the stem cells: G0/G1: 95.78%; G2: 2.61%; and S: 1.61%. These results suggest that most of the analyzed hDPSCs were in the stationary phase or slow proliferation phase. Further, the analysis revealed that the hDPSCs exhibited a high degree of multi-directional differentiation potential (see *Figure 1C*).

The induction of hDPSC differentiation into neural cells following the addition of the neural medium was also monitored by immunofluorescence and flow cytometry. After 14 days of induction, the hDPSCs were observed to be ovoid or triangular under the microscope. The associated cells varied in size and some cells were enlarged (see *Figure 2A*). The cell surfaces that protruded on both sides and the cells themselves were rich with cytoplasm. Immunofluorescence staining of GFAP and NeuN resulted in the positive staining of neurons (see *Figure 2A*). In addition, the flow cytometry analysis revealed that the precentage of nestin-positive hDPSCs increased from
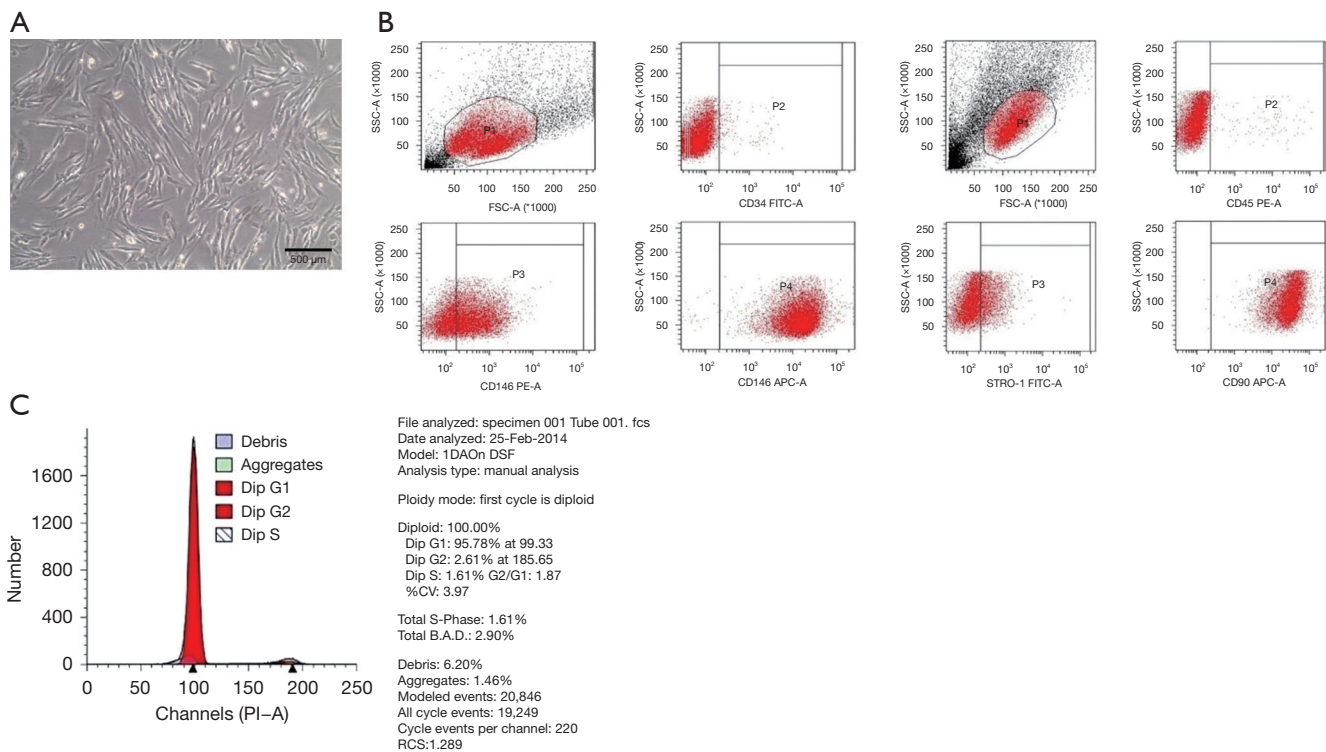
Page 6 of 12

Hu et al. PRP enhanced hDPSC neuro-regeneration

Figure 1 Characterization of multipotential hDPSCs *in vitro*. (A) Following the initial thaw, the passaged homogeneous hDPSCs grew in a monolayer with spindle-shaped morphology as observed through inverted phase contrast microscope on day 4 (×40). (B) A flow cytometry study revealed the following surface antigen expression percentages: CD34: 1.7%; CD45: 2.0%; STRO-1: 28.5%; CD146: 61.3%; and CD44: 99.6%. These results demonstrate that the hDPSCs exhibit stem cell characteristics. (C) A flow cytometry analysis of the cell cycle revealed the percentages of cells at different cell cycle stages: G1: 95.78%; G2: 2.61%; and S: 1.61%. These results suggest that most of the hDPSCs were in the stationary phase or slow proliferation phase. The results also suggest that hDPSCs have a high degree of multi-directional differentiation potential. hDPSCs, human dental pulp stem cells.

52.7% before induction to 84.4% after induction, indicating a significant increase in nestin production after induction (see *Figure 2B*).

HDPSCs combined with PRP in the treatment of spinal cord injury in rats

The acute spinal cord injury model used in this study was established as described in the Materials and Methods section. Immediately after injury, both lower extremities of the rats suddenly contracted with tail rotation. Following anesthesia, the activities of both lower limbs disappeared, and the tail could not be upturned. These rats had a BBB score of 0 points, indicating the successful establishment of the acute spinal cord injury model. Of the 45 experimental rats, 42 had a BBB score of 0, 2 had a BBB score of 9, and 1 had a BBB score of 7. Thus, the modeling success rate

was 93.3%. Notably, 2 rats died after the modeling, but no other rats had died by the end of the experiment.

A BBB open-field activity test was used to determine the recovery of the motor function of hindlimbs. Following 3 and 7 days of treatment, no significant difference in the BBB scores was observed among the 4 groups ($P > 0.05$). However, 2 weeks after treatment, the motor function of the hDPSC/PRP, hDPSC, and PRP groups was significantly more increased than that of the sham group, ($P < 0.05$). The increase was most notable in the hDPSC/PRP group. The BBB scores of the hDPSC and PRP groups were similar ($P > 0.05$). After 4 weeks, the hDPSC/PRP group had a BBB score of 10.60 ± 1.14, the hDPSC group had a BBB score of 7.20 ± 1.64, the PRP group had a BBB score of 6.40 ± 0.89, and the sham group had a BBB score of 3.60 ± 1.14 (see *Figure 3A*). The HDPSC/PRP group showed the most significant improvement in motor function compared to the
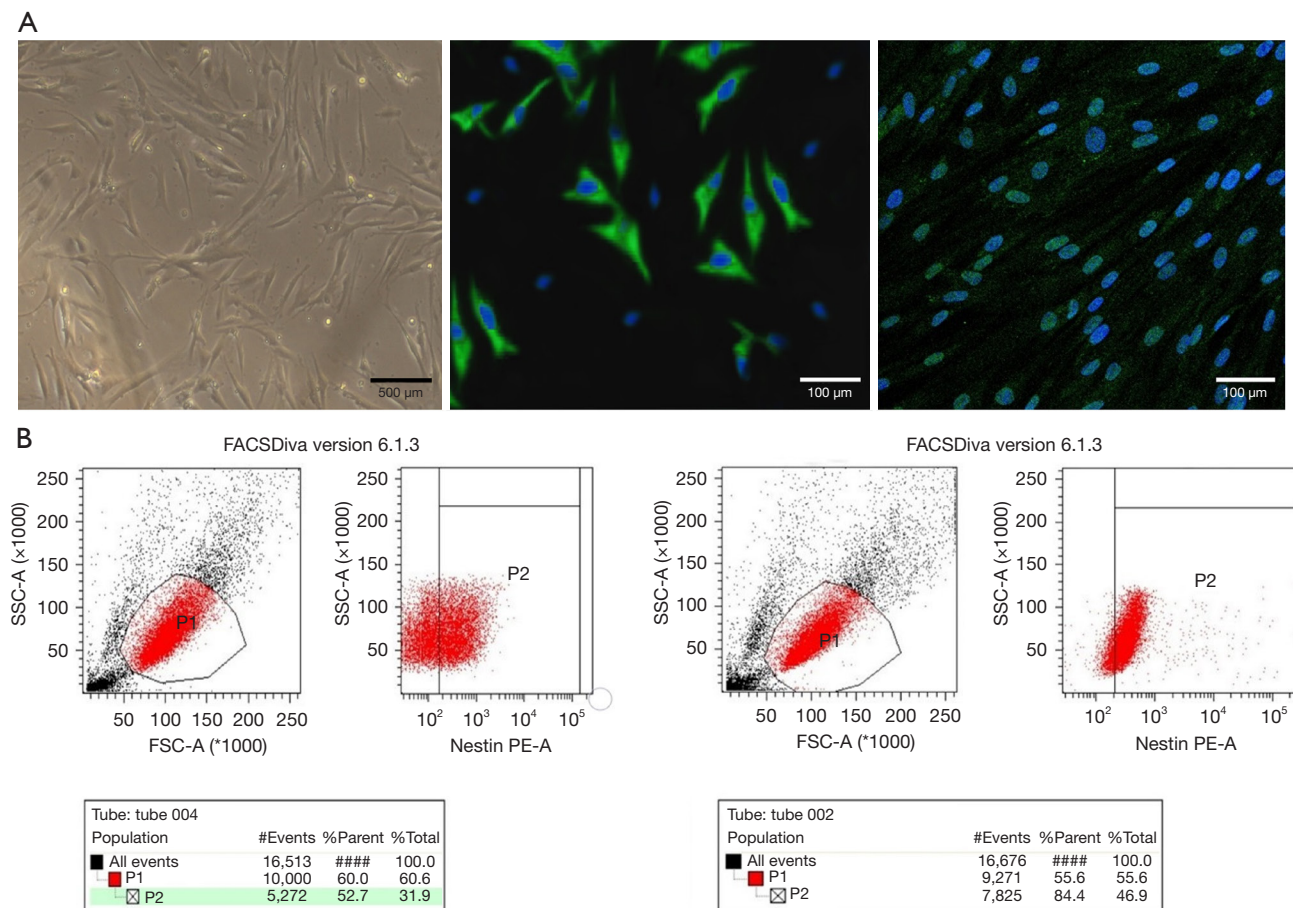
Figure 2 Neurogenic differentiation of hDPSCs *in vitro*. The induction of neurogenic differentiation of hDPSCs into neural cells following the addition of neural medium was monitored by immunofluorescence (A) and flow cytometry (B). (A) After 14 days of induction, the hDPSCs were found to be ovoid or triangular when viewed under the microscope (×40). The immunofluorescence staining of GFAP and NeuN resulted in positively stained neurons (×200). (B) A flow cytometry analysis also revealed an increase in nestin-positive hDPSCs after induction (from 52.7% before induction to 84.4% after induction), indicating a significant increase in nestin after induction. hDPSCs, human dental pulp stem cells.

hDPSC and PRP groups (P<0.05); however, there was no significant difference between the hDPSC and PRP groups (P>0.05).

To examine the pathophysiological effects of hDPSCs and PRP on spinal cord injury, pathological changes in spinal cord and syrinx formation were assessed using harvested spinal cord samples. After 4 weeks of modeling and treatment, spinal cord stenosis and scar formation were observed at the injury sites. H&E staining revealed hemorrhaging, neuronal degeneration, the infiltration of inflammatory cells, the proliferation of small blood vessels, and syrinx formation. The syrinx area encompassed 19.50%±4.80%, 26.75%±2.50%, 30.75%±3.78%, and

49.50%±6.25% of the total spinal area in the hDPSC/ PRP, hDPSC, PRP, and sham groups, respectively. The syrinx area in the HDPSC/PRP group was significantly lower than those of the other groups, especially the sham group (P<0.05). There was a significant difference between the hDPSC or PRP groups and the sham group (P<0.05); however, there was no significant difference between the hDPSC and PRP groups (P>0.05; see *Figure 3B*).

To examine the mechanisms underpinning the protective effects of hDPSCs and PRP on spinal cord injury in rats, we monitored the occurrence of apoptosis in spinal cord samples using the TUNEL assay. After 28 days of treatment, the apoptotic rate of the spinal cord cells was
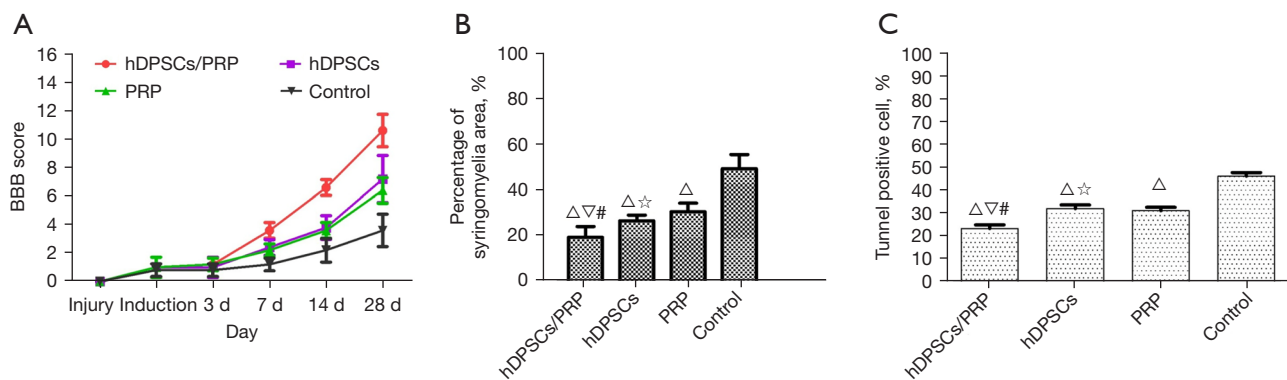
Page 8 of 12

Hu et al. PRP enhanced hDPSC neuro-regeneration

Figure 3 Pathophysiological effects of the hDPSCs/PRP double-treatment, hDPSCs single-treatment, and PRP single-treatment on spinal cord injury in the rat model. (A) Recovery of motor function determined by BBB open-field activity test. The motor function of rats from the hDPSCs/PRP group, the hDPSCs group and the PRP group showed a significant increase (P<0.05) compared to the sham group. The increase in motor function was most dramatic in the hDPSCs/PRP group. (B) Histopathological changes in spinal cord and syrinx formation. The syrinx area in the hDPSCs/PRP group was significantly lower than that in other groups, especially when compared to the sham group (P<0.05). There was a significant difference between the hDPSCs or PRP, and sham groups (P<0.05), but no significant difference was observed between the hDPSCs and PRP groups (P>0.05). (C) Apoptosis of the spinal cord determined by TUNEL assay. The hDPSCs/PRP group exhibited a significantly reduced apoptotic rate compared to the hDPSCs, PRP, and sham groups (P<0.05). The hDPSCs and PRP groups also had significantly lower apoptotic rates compared to the sham group (P<0.05); however, no significant difference was observed between the hDPSCs and PRP groups (P>0.05). hDPSCs, human dental pulp stem cells; PRP, platelet-rich plasma; BBB, Basso, Beattie, and Bresnahan. (△ compared with the control group, P<0.05; ▽ compared with hDPSCs group, P<0.05; # compared with PRP group, P<0.05; ☆ compared with PRP group, P>0.05.)

23.67%±1.52%, 32.33%±1.54%, 31.33%±1.52%, and 46.33%±1.53% in the hDPSC/PRP group, the hDPSC group, the PRP group and the sham group, respectively. The lowest apoptotic rate was observed in the hDPSC/PRP group, while the highest rate was observed in the sham group. The hDPSC/PRP group exhibited a significantly different apoptotic rate from the hDPSC, PRP, and sham groups (P<0.05). The hDPSC and PRP groups also exhibited significantly lower apoptotic rates than the sham group (P<0.05); however, no differences were observed between the hDPSC and PRP groups (P>0.05; see *Figure 3C*).

The survival and differentiation of transplanted hDPSCs in the spinal cord were also studied using immunofluorescence staining at 3 days, 2 weeks, and 4 weeks after hDPSC transplantation. HuNu expression was observed in injured spinal cords from the hDPSC/PRP and hDPSCs groups, which suggested that the transplanted hDPSCs could survive in injured spinal cord tissues (see *Figure 4*). Surviving hDPSCs were still visible in both the hDPSC groups 4 weeks after transplantation. Immunofluorescence with both HuNu-GFAP and HuNu-NeuN was also

observed in some of the neurons after 4 weeks of therapy, proving that hDPSCs can differentiate into neurons *in vivo*.

Discussion

Spinal cord injury causes neurodegenerative disease and is characterized by the degeneration of motor, sensory or autonomic neurons with concomitant loss of neural function (1). The current guidelines pertaining to the treatment of neurodegenerative diseases mainly recommend symptomatic strategies to facilitate treatment. The guidelines are predominantly based on delaying the deleterious effects resulting from the loss of neurons or neural supportive cells (4). In recent years, stem cell therapy has been proposed as a novel and promising curative strategy for the treatment of clinical conditions, including neurogenic regeneration (6,8-11). Stem cells have the potential to replace and restore impaired tissue function by differentiating into specialized cell types, including neurons. HDPSCs isolated from discarded teeth represent a rich source of adult stem cells (8-11). Multiple studies have demonstrated that hDPSCs have a number of properties,
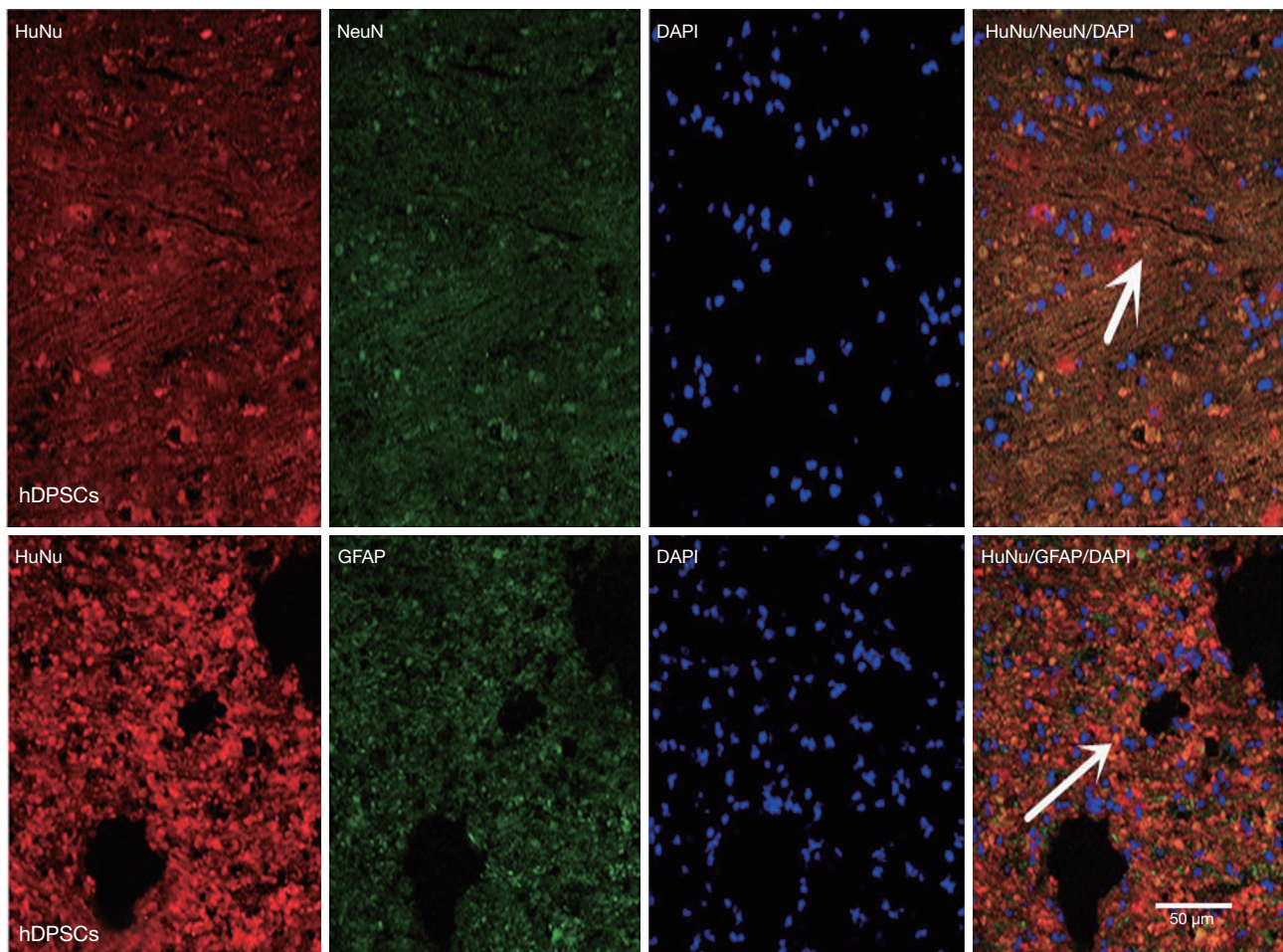
Figure 4 Survival and differentiation of transplanted hDPSCs in spinal cord by immunofluorescence staining (×400). Immunofluorescence staining was performed at 3 days, 2 weeks, and 4 weeks after hDPSC transplantation. Some of the neurons stained positive for both HuNu-GFAP and HuNu-NeuN 4 weeks after transplantation, which suggests that hDPSCs can differentiate into neurons *in vivo*. The white arrows indicate the differentiated nerve cells derived from hDPSCs. hDPSCs, human dental pulp stem cells.

including rapid proliferation, self-renewal, and multi-lineage differentiation potential. Further, these stem cells have been successfully deployed in the fields of tissue engineering and regenerative medicine. Compared with typical bone marrow MSCs, dental pulp stem cells have higher regeneration potential and proliferation ability. It is considered to be a source of stem cells with great clinical application prospects. According to more documents, dental pulp stem cells can treat spinal cord injury, Alzheimer's disease, myocardial infarction, muscular dystrophy, diabetes and immune diseases. For example, Hochuli *et al*. (19) found that neural induced deciduous tooth stem cells may be more useful for the treatment of spinal cord injury. Gazarian *et al*. (20) used okadaic acid induction to detect the therapeutic effect

of hDPSCs in the Alzheimer's disease model *in vitro*, and proved that it can significantly improve the viability of model cells and reduce apoptosis.

These latest research results provide new insights into the future clinical application of dental pulp stem cells. Dental pulp provides potential stem cell resources for clinic, is beneficial to the cell therapy of various systemic diseases, and has the potential to provide a powerful tool for regenerative medicine. At present, dental pulp stem cells can be obtained by natural deciduous teeth, isolated and expanded by professional technology, and stored in deep low temperature environment for a long time. This will undoubtedly promote the diversification of clinical application of dental pulp stem cells.

Page 10 of 12

Hu et al. PRP enhanced hDPSC neuro-regeneration

In this study, we first investigated the potential properties of *in vitro*—cultured hDPSCs via the identification of cell surface biomarkers and a cell-cycle analysis. Previous studies have identified a series of possible stem cell markers that were used as references for the characterization of hDPSCs in this study. For example, Gronthos *et al.* (7) found that hDPSCs did not express markers, including CD34 and CD45, which are normally associated with hematopoietic cells, but that hDPSCs expressed markers, such as CD44, which are normally associated with mesenchymal cells. Karaöz *et al.* (21) also compared the surface markers of hDPSCs and bone marrow-derived mesenchymal stem cells and found that the expression of CD44 and CD90 was relatively increased in hDPSCs. They also found a lower expression of CD146 in hDPSCs and a negative expression of CD34 and CD45 in both stem cell sources. Further, Suchanek *et al.* (22) found that the expression of CD29, CD44, CD90, and HLA I was increased, and the expression of CD34, CD45, CD71, and HLA II was reduced in hDPSCs.

Based on these findings, the CD44, CD90, CD14, CD34, CD45, and STRO-1 cell surface markers were used in this study to identify the stem cell properties of the cultured pulp cells. Our results revealed that CD146, CD44, and CD90 were strongly and positively expressed, STRO-1 was weakly and positively expressed, and CD34 and CD45 were negatively expressed. These results are consistent with those of previous studies (21,22), and demonstrate that isolated and cultured pulp cells display the characteristics of stem cells. We also performed a cell-cycle analysis to confirm the stem cell properties of the hDPSCs. We found that that G0/G1 phase cells accounted for 95.78% of the total cells, while the G2 phase and S phase cells accounted for the rest of the total cells (4.22%). These results are consistent with the cycle characteristics of stem cells, and prove that cells isolated from pulp tissue cells exhibit stem cell characteristics.

The neuronal differentiation of hDPSCs has been demonstrated in several *in-vitro* studies using different approaches and methods (23). In this study, after the hDPSCs were cultured in neural induction medium for 4 weeks, the hDPSCs showed morphological neurological changes, and expressed neural specific proteins (i.e., NeuN and GFAP). The flow cytometry of the induced hDPSCs showed significantly increased nestin protein expression, which proved that hDPSCs can differentiate into neural cells under certain conditions.

The successful *in-vitro* neurogenic induction of hDPSCs

prompted us to study the functional reconstruction of damaged neural tissues using induced hDPSCs *in vivo* in a rat spinal cord injury model. As part of this analysis, we observed 2 major neuro-regenerative activities in the hDPSCs. First, the hDPSCs inhibited apoptotic effects following secondary injury caused by spinal cord injury. This phenomenon resulted in a concomitant improvement in the preservation of neuronal networking. Second, the hDPSCs promoted the regeneration of neurons by replacing lost cells via differentiation into mature neurons in the spinal cord. Both neuro-regenerative activities were enhanced by the addition of PRP.

Previous studies have shown that a key aspect of cell replacement therapy in spinal cord injury treatment is the addition of neurotrophic factors. Neurotrophic factors can effectively coordinate the differentiation, survival, and apoptosis of therapeutic cells in the target area. Thus, we examined the effect of adding neurotrophic factor in rats using a double-treatment group that was treated with both hDPSCs and PRP, a single-treatment group treated with PRP, a single-treatment group treated with hDPSCs, and a sham group treated with normal saline. After treatment, a rat BBB scoring system, which was used to evaluate the motor function of the rats, revealed significant improvements in the rats in the double-treatment or single-treatment groups compared to the sham group. However, the double-treatment group exhibited a more enhanced therapeutic effect, which may be due to the interaction between hDPSCs and PRP. It may be that PRP promotes the stem cell induction of various nutrients, the regulation of the inflammatory response, and the protection of nerve cells from apoptosis. PRP contains a large number of nutritional factors that may have direct neuroprotective effects. These factors are also likely to inhibit the inflammatory response and improve the microenvironment after spinal cord injury. The possible mechanisms of PRP in the treatment of spinal cord injury are as follows: it can accelerate the growth of neuronal axons and promote nerve regeneration by producing vegetative growth factor, stimulating cell proliferation and reducing apoptosis.

Secondary injury after spinal cord injury can lead to the serious apoptosis of nerve cells. Thus, it is essential to prevent or reduce nerve cell apoptosis following injury occurrence. Neuronal apoptosis is an important part of the pathological mechanism of secondary spinal cord injury. Inhibiting neuronal apoptosis can not only reduce the secondary spinal cord injury, but also promote the recovery of spinal cord nerve function. Methods to inhibit

neuronal apoptosis include drug inhibition methods, such as erythropoietin, riluzole, Chinese Mongolian medicine, and physical inhibition methods, such as acupuncture and hyperbaric oxygen therapy. A previous study demonstrated that pulp tissue transplanted to half-cut spinal cords from a spinal cord injury model can increase the survival of neuronal cells and reduce apoptosis. This finding may be related to the release of nutritional factors from the pulp tissues (24). Another study reported that following the transplantation of dental pulp stem cells to half-cut spinal cord injury sites, hDPSCs facilitate the protection of neurons from cell apoptosis (25). Our study revealed that hPPSCs combined with PRP better protect neurons from apoptosis.

The transplantation of hDPSCs into the injured rat spinal cord caused the marked recovery of hind-limb locomotor functions. However, these results may also have been caused by neurogenic differentiation following the addition of PRP. In this experiment, we were able to promote the survival and neurogenic differentiation of transplanted hDPSCs. Our results revealed that the stem cells survived in the injured area at 3 days after transplantation, and the survival effect lasted for 4 weeks. Additionally, an immunofluorescence double-labeling analysis proved that hDPSCs differentiate into nerve cells *in vivo*. Our experiments showed that rats treated with hDPSCs combined with PRP displayed greater neurogenic differentiation and better survival than rats in the sham group.

In summary, this study demonstrated, for the first time, that a combination of hDPSCs and PRP protects neurons from apoptosis and facilitates differentiation into neuronal cells both *in vitro* and in the rat spinal cord. This approach is likely to be invaluable in the future of regenerative medicine. Thus, our study provides a promising approach that paves the way for a highly effective hDPSC-based therapy in the treatment of central nervous system disorders.

Acknowledgments

Footnote

Ethical Statement: The authors are accountable for all aspects of the work in ensuring that questions related to the accuracy or integrity of any part of the work are appropriately investigated and resolved. Animal experiments were performed under a project license (No. GDY1602042) granted by the institutional ethics committee of Guangdong Medical University (Zhanjiang, China), in compliance with national guidelines for the care and use of animals.

References

1. Reier PJ. Cellular transplantation strategies for spinal cord injury and translational neurobiology. NeuroRx 2004;1:424-51.
2. Noonan VK, Fingas M, Farry A, et al. Incidence and prevalence of spinal cord injury in Canada: a national perspective. Neuroepidemiology 2012;38:219-26.
3. Case LC, Tessier-Lavigne M. Regeneration of the adult central nervous system. Curr Biol 2005;15:R749-53.
4. Bradbury EJ, McMahon SB. Spinal cord repair strategies: why do they work? Nat Rev Neurosci 2006;7:644-53.
5. Furlan JC, Noonan V, Singh A, et al. Assessment of impairment in patients with acute traumatic spinal cord injury: a systematic review of the literature. J Neurotrauma 2011;28:1445-77.
6. Horner PJ, Gage FH. Regenerating the damaged central nervous system. Nature 2000;407:963-70.
7. Gronthos S, Mankani M, Brahim J, et al. Postnatal human

Page 12 of 12

Hu et al. PRP enhanced hDPSC neuro-regeneration

dental pulp stem cells (DPSCs) in vitro and in vivo. Proc Natl Acad Sci U S A 2000;97:13625-30.

8. Nuti N, Corallo C, Chan BM, et al. Multipotent Differentiation of Human Dental Pulp Stem Cells: a Literature Review. Stem Cell Rev Rep 2016;12:511-23.

9. Király M, Porcsalmy B, Pataki A, et al. Simultaneous PKC and cAMP activation induces differentiation of human dental pulp stem cells into functionally active neurons. Neurochem Int 2009;55:323-32.

10. Arthur A, Rychkov G, Shi S, et al. Adult human dental pulp stem cells differentiate toward functionally active neurons under appropriate environmental cues. Stem Cells 2008;26:1787-95.

11. Gong T, Heng BC, Lo EC, et al. Current Advance and Future Prospects of Tissue Engineering Approach to Dentin/Pulp Regenerative Therapy. Stem Cells Int 2016;2016:9204574.

12. Kawano H, Kimura-Kuroda J, Komuta Y, et al. Role of the lesion scar in the response to damage and repair of the central nervous system. Cell Tissue Res 2012;349:169-80.

13. Sayer FT, Oudega M, Hagg T. Neurotrophins reduce degeneration of injured ascending sensory and corticospinal motor axons in adult rat spinal cord. Exp Neurol 2002;175:282-96.

14. Weissmiller AM, Wu C. Current advances in using neurotrophic factors to treat neurodegenerative disorders. Transl Neurodegener 2012;1:14.

15. Tobita M, Tajima S, Mizuno H. Adipose tissue-derived mesenchymal stem cells and platelet-rich plasma: stem cell transplantation methods that enhance stemness. Stem Cell Res Ther 2015;6:215.

16. Civinini R, Macera A, Nistri L, et al. The use of autologous blood-derived growth factors in bone regeneration. Clin Cases Miner Bone Metab 2011;8:25-31.

17. Martínez CE, Smith PC, Palma Alvarado VA. The influence of platelet-derived products on angiogenesis and tissue repair: a concise update. Front Physiol 2015;6:290.

18. Barros Filho TE, Molina AE. Analysis of the sensitivity and reproducibility of the Basso, Beattie, Bresnahan (BBB) scale in Wistar rats. Clinics (Sao Paulo) 2008;63:103-108.

19. Hochuli AHD, Senegaglia AC, Selenko AH, et al. Dental Pulp from Human Exfoliated Deciduous Teeth-derived Stromal Cells Demonstrated Neuronal Potential: In Vivo and In Vitro Studies. Curr Stem Cell Res Ther 2021;16:495-506.

20. Gazarian K, Ramirez-Garcia L, Tapía Orozco L, et al. Human Dental Pulp Stem Cells Display a Potential for Modeling Alzheimer Disease-Related Tau Modifications. Front Neurol 2021;11:612657.

21. Karaöz E, Demircan PC, Sağlam O, et al. Human dental pulp stem cells demonstrate better neural and epithelial stem cell properties than bone marrow-derived mesenchymal stem cells. Histochem Cell Biol 2011;136:455-73.

22. Suchanek J, Soukup T, Visek B, et al. Dental pulp stem cells and their characterization. Biomed Pap Med Fac Univ Palacky Olomouc Czech Repub 2009;153:31-5.

23. Taghipour Z, Karbalaie K, Kiani A, et al. Transplantation of undifferentiated and induced human exfoliated deciduous teeth-derived stem cells promote functional recovery of rat spinal cord contusion injury model. Stem Cells Dev 2012;21:1794-802.

24. Montgomery CT, Tenaglia EA, Robson JA. Axonal growth into tubes implanted within lesions in the spinal cords of adult rats. Exp Neurol 1996;137:277-90.

25. Nosrat IV, Widenfalk J, Olson L, et al. Dental pulp cells produce neurotrophic factors, interact with trigeminal neurons in vitro, and rescue motoneurons after spinal cord injury. Dev Biol 2001;238:120-32.